ACS ES&T Engineering

pubs.acs.org/estengg

Article

Quantitative Proteomics and Quantitative PCR as Predictors of *cis*-1,2-Dichlorethene and Vinyl Chloride Reductive Dechlorination Rates in Bioaugmented Aquifer Microcosms

Mandy M. Michalsen, Fadime Kara Murdoch, Frank E. Löffler, John Wilson, Paul B. Hatzinger, Jack D. Istok, Larry Mullins, Amy Hill, Robert W. Murdoch, Charles Condee, and Katarzyna H. Kucharzyk*

Cite This: *ACS EST Engg.* 2022, 2, 43−53

Read Online

ACCESS | Metrics & More | Article Recommendations | Supporting Information

ABSTRACT: Quantitative measurement of process-specific biomarker genes of *Dehalococcoides mccartyi* (*Dhc*) supports monitoring at chlorinated ethene contaminated sites. In this study, we varied *Dhc* cell abundances from ~10^3 to 10^8 cells/mL in aquifer microcosms and correlated the corresponding reductive dehalogenase (RDase) gene and RDase protein abundances with measured reductive dechlorination (RD) rates of *cis*-1,2-dichloroethene (cDCE) and vinyl chloride (VC). An additional set of microcosms tested the RD rate-predictive power of the regression analyses. These efforts revealed (1) that targeted proteomics quantifies *Dhc* biomarker proteins (e.g., TceA and VcrA, OmeA) over a relevant range of *Dhc* cell densities, and (2) that protein and gene abundances can predict RD rates. Protein detection limits translated to a rate coefficient of 10^{-4} day^{-1} (0.04 year^{-1}) for both k_{cDCE} and k_{vc}, which is within the range observed at sites undergoing monitored natural attenuation (MNA) (i.e., without the implementation of enhanced bioremediation treatment). Rates predicted using a combination of quantitative biomarker gene and protein measurements generally resulted in the best match with experimentally determined rate constants. These new findings provide evidence that quantitative biomarker measurements may be useful predictors of *in situ* RD rates, which would constitute a major advance for the cost-effective management of contaminated sites.

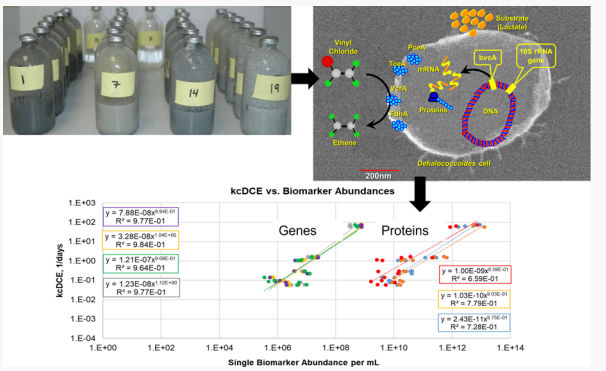

KEYWORDS: *reductive dechlorination, bioremediation, quantitative qPCR, quantitative proteomics, reductive dehalogenase*

Downloaded via 188.192.25.150 on January 24, 2022 at 18:20:37 (UTC).
See https://pubs.acs.org/sharingguidelines for options on how to legitimately share published articles.

INTRODUCTION

Groundwater aquifers impacted with chlorinated solvents, specifically chlorinated ethenes, threaten drinking water supplies worldwide. Thus, cost-effective remedial approaches are needed to address this widespread contamination. Monitored natural attenuation (MNA) has been widely used, often in conjunction with source remediation.[1] The acceptance of MNA as the selected site remedy requires a quantitative prediction of the future distribution of the target contaminant(s). This is typically achieved by calibrating a groundwater model to the specific site conditions. Thus, the contribution of biodegradation to contaminant loss is conventionally described using a pseudo-first-order rate constant for each contaminant.[2,3] These rate constants can be extracted from long-term monitoring data. Unfortunately, at many sites, there are either not enough sampling locations (i.e., groundwater wells) or the sampling duration is inadequate to constrain the rate constants to meaningful values. A surrogate rate constant can be extracted from microcosm studies, but such studies are expensive, require many months to conduct, and may not adequately represent *in situ* conditions. The ability to infer degradation rate constants of *cis*-1,2-dichloroethene (cDCE) and vinyl chloride (VC) from the abundance of nucleic acids or protein biomarkers would represent a significant advance in the application of MNA at sites where degradation rates are either not available or are poorly constrained.

In situ bioremediation of chlorinated ethenes has emerged as a robust technology and has been implemented at many sites via biostimulation with an electron donor. Often, biostimulation is complemented with bioaugmentation with commercial microbial cultures such as consortium SDC-9.[4] The micro-

Received: June 7, 2021
Revised: October 25, 2021
Accepted: November 1, 2021
Published: November 16, 2021

© 2021 American Chemical Society

https://doi.org/10.1021/acsestengg.1c00207
ACS EST Engg. 2022, 2, 43−53

biology of reductive dechlorination (RD) of chlorinated ethenes to non-toxic ethene is fairly well understood, and qPCR assays targeting biomarker genes of keystone bacteria, in particular *Dehalococcoides mccartyi* (*Dhc*), involved in the reductive dechlorination of tetrachloroethene (PCE) or trichloroethene (TCE) through cDCE to VC to ethene, are available.[5,6] Other than reductive dehalogenase (RDase) genes, a newly identified protein complex included in the organohalide respiration molybdoenzyme (OmeA), formally called the complex iron−sulfur cluster molybdoenzyme (CISM), is found to have hydrogenase activity.[7] The value of quantitative polymerase chain reaction (qPCR) targeting the *Dhc* 16S rRNA gene and the VC RDase genes *vcrA*, *bvcA*, and *tceA* as diagnostic and prognostic site assessment and bioremediation monitoring tools has been demonstrated.[2,3] A potential drawback of DNA-based qPCR is the presumption that inactive (i.e., non-dechlorinating) *Dhc* cells would potentially be enumerated but without contributing to reductive dechlorination activity. The measurement of gene transcripts (i.e., mRNA) of functional biomarker genes via reverse transcription-qPCR (RT-qPCR) can potentially enumerate metabolically active cells, and thus be a more direct measure of reductive dechlorination activity.[8] Unfortunately, low transcript levels in *Dhc* cells[9] and the difficulty of quantitatively extracting labile RNA from environmental matrices are major challenges, and the RT-qPCR approach so far has limited utility for monitoring RD activity.

Recent advances in proteomics allow the quantitative measurement of biomarker proteins such as the *Dhc* RDases VcrA and TceA, both of which have been implicated in reductive dechlorination of cDCE and VC to environmentally benign ethene[10,11] and OmeA that has a potential function as an electron-channeling module between the Hup hydrogenase and the reductive dehalogenase.[12] Since the turnover of contaminant (e.g., cDCE) should correlate with the amount of catalyst (i.e., *Dhc* cells with RDases), we hypothesize that quantitative proteomics (qProt) data can be used to predict process rates. If this is proven, qProt could complement the current gene-centric qPCR approach for monitoring sites undergoing MNA or enhanced bioremediation treatment.

To evaluate if quantitative measurements of *Dhc* biomarker genes (i.e., qPCR) and proteins (i.e., qProt) correlate with RD rates, microcosms with contaminated site aquifer material were bioaugmented with consortium SDC-9 to establish initial abundances of *Dhc* cells ranging from ~10^3 to 10^8 *Dhc* cells per mL. RD rate constants were calculated from the observed changes in concentrations of cDCE and VC over time in the microcosms, and correlation analysis with qPCR and qProt data was performed.

MATERIALS AND METHODS

Aquifer Solids and Groundwater. Aquifer material was collected from the chlorinated volatile organic compound (cVOC)-contaminated zone of the Joint Base Lewis McCord (JBLM) Landfill 2 (LF) (Tacoma, WA). The description of sampling is detailed in the Supporting Information (SI). Additional aquifer material for metagenomics was collected at Former Lordstown Ordnance Depot (FLOD) (Lordstown, OH) and Naval Air Station North Island, Installation Restoration Site 5 (NASNI IR Site 5) (San Diego, CA), and Naval Air Station North Island, Installation Restoration Site 9 (NASNI IR Site 9) (San Diego, CA).

Growth of SDC-9. The SDC-9 consortium was grown in reduced anaerobic mineral medium (RAMM) in a 4000 L fermenter amended with lactate as a carbon source and electron donor, PCE as the sole electron acceptor, and yeast extract as a nutrient source following previously described procedures.[4] For the current studies, culture suspension was removed from the fermenter, centrifuged, and suspended in RAMM to a *Dhc* cell density of ~1×10^{10} cells/mL based on optical density (OD), α = 600 nm[13]. The culture was then diluted for addition to microcosms as described below. Initial studies were conducted to estimate biodegradation rates of cDCE by the SDC-9 prior to microcosm preparation and are discussed in Kucharzyk et al., 2020.[14]

Microcosm Study #1. Four sets of triplicate treatments were prepared inside a Coy environmental chamber with a 100% N_2 headspace (no H_2 gas). Sterile 500 mL amber glass analytical bottles with Teflon-lined septa screw caps were used to prepare microcosms. Each bottle contained site groundwater (475 mL) that had all cVOCs removed by nitrogen sparging, sodium lactate (500 mg/L final concentration), and sodium bromide (10 mg/L as Br^-). Bromide was used as a conservative tracer to document losses of VOCs and fatty acids due to dilution as all water in the bottles was replaced with VOC- and VFA-free site water after sample collection. SDC-9 culture was then diluted into triplicate microcosm bottles to achieve final *Dhc* densities of 10^8 cells/mL, 10^7 cells/mL, 10^6 cells/mL, and 10^5 cells/mL. Solid $CaCO_3$ (1 g) was added to buffer the pH of each microcosm during incubation following spiking with cDCE (5 mg/L final concentration). Additional groundwater was added so that <1 mL headspace remained in bottles, which were then sealed and removed from the anoxic chamber. Each bottle was incubated at 15 °C on a bottle roller (~0.5 rotations per minute) prior to sampling for analysis of cDCE and other parameters. Live controls consisted of site groundwater amended with cDCE, NaBr, and sodium lactate. Killed controls were prepared by spiking site groundwater with cDCE, NaBr, sodium lactate, and 500 mg/L $HgCl_2$. No SDC-9 was added to the live or killed controls.

Microcosm Study #2. Three sets of treatments were prepared in clean, sterile 1000 mL glass Boston round bottles. All microcosms were amended with 500 mg/L sodium lactate, 5 mg/L cDCE, and 10 mg/L Br^- as described. Microcosms received SDC-9 to achieve estimated final densities of 10^7 *Dhc*/mL or 10^6 *Dhc*/mL in microcosm bottles using the preparation and dilution method described above. Control microcosm sets M2-1 and M2-2, received only sparged groundwater. Live microcosms (set M2-3) received 353 g of aquifer solids at 15% moisture content (300 g dry weight). After all amendments had been added, the microcosms were filled with nitrogen-sparged site groundwater, sealed, and placed on a bottle roller (1 rpm) at 15 °C. After 10 days of incubation, 2.0 g of solid $CaCO_3$ was added to maintain a circumneutral pH. Live controls and killed controls were constructed as described above using bottles that contained groundwater and sediment.

Microcosm Study #3. Microcosms in study #3 were prepared to evaluate whether the initial decline in pH in some of the microcosms in study #2 affected degradation kinetics. Microcosms in set M3-1 were created using the same conditions as set M2-1, and microcosms in set M3-2 were created using the same conditions as set M2-3, except that 2.0 g of $CaCO_3$ was added when the microcosms were initially prepared.

https://doi.org/10.1021/acsestengg.1c00207
ACS EST Engg. 2022, 2, 43−53

Microcosm Sampling. All microcosms were sampled inside a Coy environmental chamber with a N_2 headspace. Liquid samples were removed from the microcosms with gastight syringes and transferred to appropriate sample containers. Sample volumes consisted of the following: 2 mL for cDCE and VC (EPA Method 8260B); 4 mL for methane, ethane, and ethene (EPA Method 3810/RSK-175); 1 mL for anions (EPA Method 300[13]) and volatile fatty acids (modified EPA Method 300[13]); and 5 mL for pH determination. Duplicate 15 mL aqueous samples, one for qPCR and the other for qProt analysis, were removed using a glass pipette and transferred to sterile plastic screwcap 50-mL conical tubes. Cells were collected by centrifugation for 40 min at 10,000 rpm using a refrigerated Sorvall Lynx 6000 centrifuge and a F21-8x50y rotor (Thermo Scientific). Immediately after centrifugation, the supernatant was aspirated from the cell pellets and the samples were frozen at −80 °C. Nitrogen-purged site groundwater was added to the microcosms to replace the water removed during sampling, punctured septa were replaced, and then the bottles were returned to the rollers. Samples from the microcosm treatments were collected at different intervals based on the initial *Dhc* cell abundances. Sampling of microcosms containing aquifer material was conducted as described above, except that the bottles were removed from the rollers for 30 min to allow solids to settle prior to liquid sampling. Samples for qPCR and qProt analyses were collected and analyzed at select time points representing the beginning, middle, and end of the incubation periods and the extent of the cDCE and VC degradation.

DNA Extraction and qPCR. DNA was isolated from cell pellets with DNeasy PowerLyzer PowerSoil Kit (Qiagen) according to the manufacturer's instructions with bead-beating (OMNI Bead Ruptoer, 5 m/s for 3 min) (OMNI International) to enhance cell lysis. DNA was eluted into nuclease-free water and the concentration was determined with a Qubit fluorometer (Invitrogen) using double stranded DNA (dsDNA) Broad-Range assay kit according to the manufacturer's instructions. DNA was stored at −80 °C until analysis.

The abundance of total bacterial 16S rRNA genes, *Dhc* 16S rRNA genes, and *tceA* and *vcrA* genes were determined using previously reported TaqMan qPCR assays.[15−17] New primer and probe combination sets were designed for the *pceA* gene (SDC9_448350) and the *omeA* of *Dhc*. *pceA* encodes for an RDase implicated in PCE and TCE RD to cDCE. *omeA* is an essential electron transfer protein of the RD protein complex in *Dhc*.[12,18] Primer and probe sequences are summarized in Tables S1 and S2.

qPCR was performed using the QuantStudio 12 K Flex Real-Time PCR system (Applied Biosystems [AB]). Every 10 μL reaction consisted of 5 μL of 2 × Taqman Universal PCR Master Mix (AB), 2 μL of diluted (1:10 and 1:100) DNA template, and forward and reverse primers and probe at final concentrations of 300 nM each. Reactions were initially held for 2 min at 50 °C and 10 min at 95 °C following 40 cycles of denaturation at 95 °C for 15 s and annealing and extension at 60 °C for 1 min. The qPCR results were analyzed using the QuantStudio 12 K Flex Real-Time PCR System Software (AB).

Metagenome Sequencing and Assembly. Extracted DNA samples were sequenced on an Illumina NovaSeq 6000 S1 150 bp paired end flow cell with a target read depth of 37.5 million read pairs per sample. QA/QC and metagenome assembly were performed using the KBase system.[19] Reads were trimmed using Trimmomatic v0.36 with a 4 bp sliding window and PHRED threshold of 30.[20] Resulting paired-end reads were taxonomically classified using Kaiju v1.7.3[21] and assembled using metaSPAdes v3.13.0 with a minimum contig size of 2000 bp and default kmer settings.[22] The resulting assemblies were characterized using QUAST v4.4.[23] The detailed methods are described in the SI.

Detection of *Dhc omeA* Genes. The presence of *Dhc* OmeA was determined by searching all proteins against a custom *Dhc*-OmeA HMM model created from the 30 OmeA proteins found in each of the 30 isolate *Dhc* genomes available in the Integrated Microbial Genomes database[24] as detected by annotation with TIGR01553. Only one *omeA* gene was identified in each available *Dhc* genome. The HMM search was conducted with default thresholds using HMMER v3.3.2.

Assessment of Applicability of qProt Assays to Sample Specific RDase Alleles. Specificity of qProt assay peptides for VcrA, TceA RDases, and OmeA was determined by conducting a BlastP search of the qProt peptide sequences against a database consisting of all non-redundant respiratory RDases detected in the samples. Only full-length 100% matches were considered as positive hits.

Quantitative Proteomics (qProt). Samples collected during the microcosm study were frozen at −80 °C and shipped on dry ice to Battelle for proteomic analysis. Proteins were extracted, spiked with a cocktail of 250 fmol/μL isotopically labeled peptides (Table S3), digested, and purified using previously developed methods.[10] Bovine serum albumin (BSA) was used to monitor digestion efficiency. The indexed retention time (iRT) peptide cocktail (Sciex) was used to monitor instrument performance. Following digest downstream processing, 10 μL of sample was injected into the Xevo TQ-XS triple quadrupole mass spectrometer (Waters).

Mass spectrometric parameters for the analysis of target proteins on the Xevo TQ-XS triple quadrupole mass spectrometer were optimized for *Dhc* biomarker peptides.[10] Isotopically labeled peptides were injected via syringe infusion, and precursor-to-product ion transitions were identified and optimized using the IntelliStart feature in MassLynx v4.2 software. All determined parameters for the isotopically labeled peptides were then used for their corresponding native peptides. An unscheduled selected reaction monitoring (SRM) method was created using the top two most abundant transitions for each target peptide. Sample MS/MS data were acquired using an Acquity M-class liquid chromatograph system (Waters) directly connected to a Xevo TQ-XS mass spectrometer. Detailed description of parameters is provided in the SI.

Rate Constants for Reductive Dechlorination of cDCE and VC. First-order RD rate constants for cDCE and VC (k_{cDCE} and k_{VC}) in the microcosms were estimated by fitting a numerical approximation of the first order reaction equations for sequential degradation of cDCE to VC, and then to ethene, to the change in molar concentrations of cDCE, VC, and ethene (target compounds). The Microsoft Excel Solver was used to minimize the sum of squared error between the measured and model-estimated values to obtain the best fit.

Removal of water in the microcosms for sampling and its replacement caused dilution of cDCE, VC, and ethene. A dilution correction factor was applied at each sampling point by dividing the total moles of target compound(s) present in the microcosm by the total moles of target compound(s) present at time zero. Br^- was added to the microcosms to

https://doi.org/10.1021/acsestengg.1c00207
ACS EST Engg. 2022, 2, 43−53

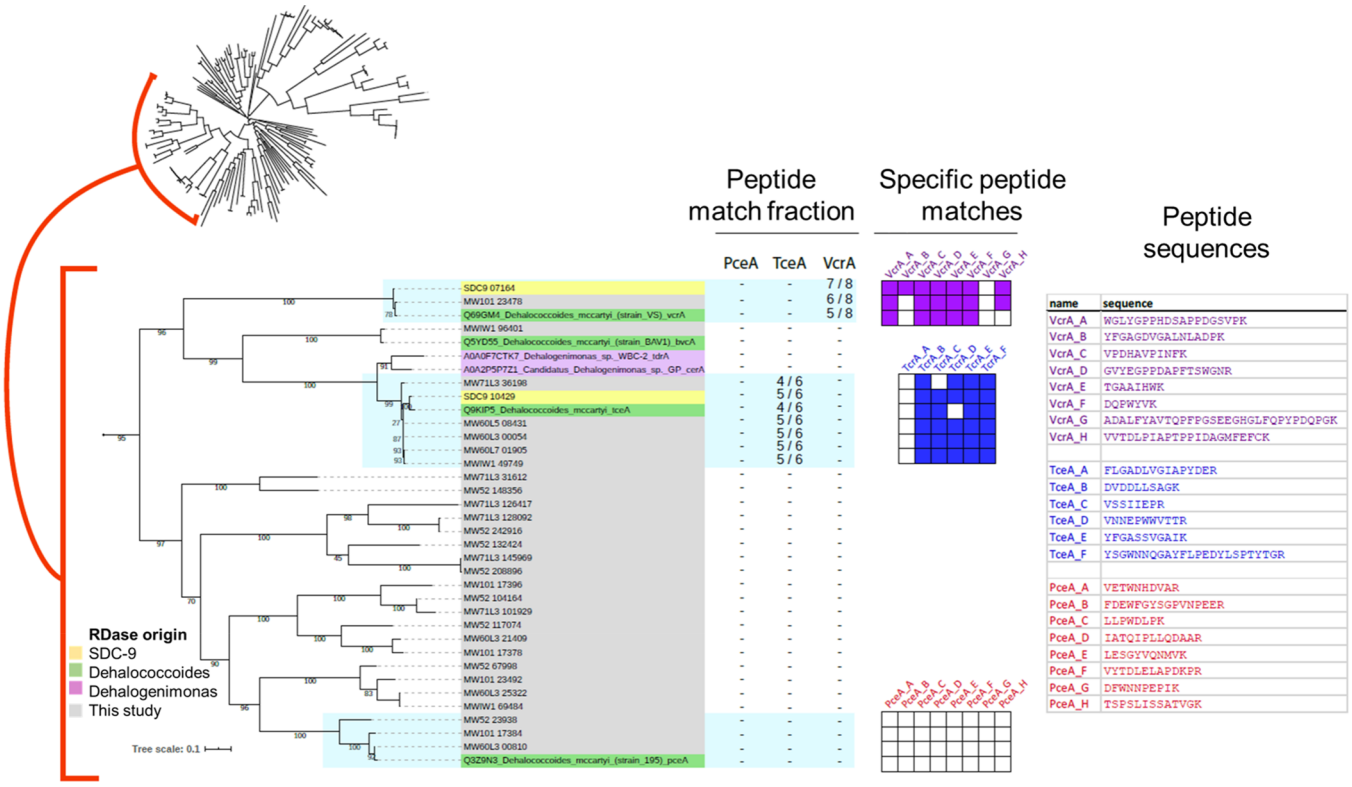

Figure 1. Relationships of putative TceA, VcrA, and *Dhc*-like PceA proteins identified in samples from selected contaminated sites with reference *Dhc* (green) and *Dehalogenimonas* (purple) RDases. "Peptide match fraction" is the number of targeted peptides 100% aligned to the indicated RDase. The light blue rectangles indicate a proposed range for the designation of alleles of a particular gene (*pceA*, *tceA*, or *vcrA*). This designation is supported by the derived phylogenetic relationship (i.e., tree structure) and by peptide matching of TceA and VcrA. "Specific peptide matches" define peptide matching to the original qProt peptide set. The lack of any matches to the *Dhc*-like PceA alleles is expected given that these peptides were designed based on a *Dehalobacter*/*Desulfitobacterium* clade PceA identified in SDC-9. The "rectangular" tree is an enlargement of the indicated section of the global RDase tree (Figure S1), focused on putative site-specific TceA, VcrA, and *Dhc*-like PceA.

correct for dilution losses of cDCE, VC, and ethene. Measured concentrations of target compounds were multiplied by the initial concentration of Br^- and then divided by the actual (measured) Br^- concentration in the vessel. Dilution correction based on measured Br^- concentrations yielded similar results to the correction based on total moles of target compounds.

In the bottles with aquifer material, some mass of the target compounds was removed by sorption to the solids. In these treatments, the rate constants were calculated based on the change in the total amount of each target compound in the bottles over time. Assuming linear partitioning, eq 1 can be used to calculate the total mass of each target compound in the bottle.

$$M_{(\text{tot,sorption corrected})} = C_w V_w + C_w M_s (0.63 K_{ow} f_{oc}) \quad (1)$$

where $M_{(\text{tot,sorption corrected})}$ is the mass of the target alkene, *Cw* is the dilution-corrected molar concentration in water, *Vw* is the volume of water present in the bottle, *Ms* is the mass of solids in the bottle, *Kow* is the VOC-specific octanol–water partitioning coefficient, and *foc* is the fraction of organic carbon associated with the solids, which was assumed to be 0.001.[25] *Kow* values used for cDCE, VC, and ethene were 72.4, 28.8, and 13.5, respectively.[26] Rate coefficients for each test replicate microcosm were determined separately using this approach. The 95% confidence interval associated with each fitted rate constant was determined following an established approach.[27]

Correlating Reductive Dechlorination Rates and Biomarker Abundances. Log-transformed rate coefficients and biomarker abundances were subject to the Shapiro–Wilk normality test.[28] The Spearman Rank Order Correlation analysis followed by ordinary least squares regression (OLSR) analysis was used to quantify the relationship between biomarker abundances and rate coefficients. Rate coefficients represent an integrated measure of activity in each microcosm over time, whereas biomarker abundances provide a single measure at various time points during the incubation. Correlation analysis was performed twice: once using the global data sets, which included biomarker abundances collected at early, mid, and late time points from each microcosm with the corresponding integrated rate coefficients measured for that microcosm, and again using only mid-point biomarker abundances and the corresponding rate coefficients.

Assessing Predictive Power of Biomarker Abundances. The microcosm experiments were divided into a "training set" and an "evaluation set." Rate coefficients and biomarker abundances from the "training set" microcosms were subject to OLSR analysis of rate constants on abundance. Only data from microcosms where the rate coefficients were greater than zero at 95% confidence were included in the analysis. Measured biomarker abundances in the "evaluation set" of microcosms were entered as the "*x*" variable in the regression equations to obtain a predicted rate coefficient. The predicted rate coefficient was then compared to the measured rate coefficient for the "evaluation set" microcosms. Two types of training sets

https://doi.org/10.1021/acsestengg.1c00207
ACS EST Engg. 2022, 2, 43–53

were established. The first training set featured randomly selected microcosms that contained either 10^6, 10^7, or 10^8 *Dhc* cells/mL. The second training set featured the global average of biomarker abundances and rate coefficients for all microcosms at all time points that contained either 10^6, 10^7, or 10^8 *Dhc* cells/mL. The predictive power of the quantitative biomarker analysis was evaluated by comparing: (1) the measured vs predicted rate constants for each individual biomarker, (2) the measured vs the average of the predicted rate constants for the various gene biomarkers, (3) the measured vs the average of the predicted rate constants for the various protein biomarkers, and (4) the measured vs the average of the predicted rate constants for gene and protein biomarkers.

Data Availability. Metagenome shotgun sequencing reads are available in the NCBI Sequencing Read Archive under accession numbers SRR16297622 to SRR16297629. *rdhA* and *omeA* gene alleles are available in GenBank under accession numbers OK528336 to OK528509 and OK528330 to OK528335, respectively.

RESULTS AND DISCUSSION

Allelic Variation of RDases in Groundwater from Contaminated Sites. Metagenome sequencing allowed us to determine if the current qProt assay, based on the metagenome of the SDC-9 culture, is suitable for quantifying *Dhc* proteins in samples from cVOC-contaminated field sites. While the sequence space of the relevant *Dhc* RDase genes is tightly constrained,[29] this analysis was performed to define specificity of the existing qProt assay to inform its customization.

Groundwater samples from FLOD (MW101) and IR Site 9 (MW52, MW60L3, MW60L5, MW60L7, MW71L3, MW74L3, and MWIW1) rendered eight metagenomes clustered at 100% amino acid identity. A total of 109 unique RDases comprising a larger sequence space than the reference RDases were identified (Figure S1), and 30 reference respiratory RDases and the 12 RDases found in SDC-9 were reconstructed.[14] Alignment of these peptides to the RDases revealed that the largest proportions of peptides matched the original SDC-9 targets. Five closely related TceA proteins and one VcrA protein were identified in metagenomes from this study (Figure 1). No PceA peptide matches to any of the FLOD/IR Site 9 RDases were detected, nor were there any FLOD/IR Site 9 RDases even moderately related to any PceA protein from the *Dehalobacter/Desulfitobacterium* clade. However, there were some close relatives to a *Dhc* PceA protein (*Dhc mccartyi*), which was not present in SDC-9 and is not covered by the current qProt assay. The SDC-9 metagenome showed the opposite pattern, with several *Dehalobacter/Desulfitobacterium* clade *pceA* genes but no *Dhc*-like *pceA* genes.

In conclusion, the respiratory RDase genes identified in the sampled metagenomes were not identical to any reference RDase gene or to any SDC-9 RDase gene. Only 1 *vcrA* and 5 *tceA* alleles were identified across the FLOD/IR Site 9 metagenomes. The *vcrA* allele matches with six of the target peptides, and the *tceA* alleles match with for or five, more than sufficient for accurate and sensitive quantification. In both cases, the peptide specificity is very similar or identical to that shown by the SDC-9-derived alleles. While the current qProt RDase assays did not detect the PceA proteins present at the test sites, PceA does not perform a critical or rate-limiting step in the dechlorination reaction, and thus it was excluded from subsequent analyses.

Assembly of site-specific variants of the *omeA* gene led to the detection of a single *omeA* gene in six of the eight metagenomes. The existing OmeA qProt assay employs 10 peptides for quantification which match 100% to the OmeA protein detected in five of the metagenomes (from IR Site 9 wells MW52, MW60L3, MW60L5, MW60L7, and MW1W1), although the final OmeA, from FLOD well MW101, only matched 3 of the 10. Overall, the site-specific metagenome analysis demonstrated that the current qProt SDC-9 assay is suitable for the quantification of TceA, VcrA, and OmeA proteins present at other environmental sites contaminated with chlorinated solvents.

Dechlorination of cDCE in Microcosms Inoculated with Varied Titers of *Dhc* Cells. RD of cDCE to VC and ethene was observed in the all microcosms inoculated with the SDC-9 culture. cDCE RD did not contribute to meaningful cDCE degradation in killed and live control microcosms, indicating that indigenous biotic or abiotic processes did not contribute to cDCE degradation. In microcosms inoculated with SDC-9, lactate was consumed with the concomitant increase in acetate and propionate concentrations, which then declined slowly over time (Figures S2–S14 in the SI). Examples showing the measured and model-fitted time-series cDCE, VC, and ethene concentrations from representative microcosm sets are shown in Figure 2.

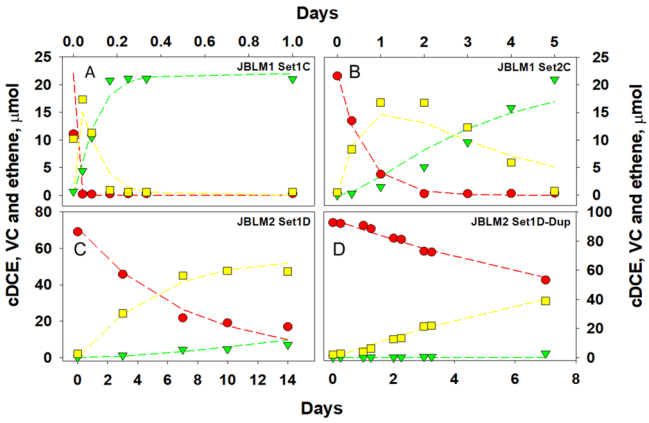

Figure 2. Measured and model-fitted cDCE, VC, and ethene concentrations in microcosms: (A) JBLM set 1C, (B) JBLM1 set 2C, (C) JBML2 set 1D, and (D) JBML2 set 1D-Dup. Measured (symbols) and fitted (dashed lines) time-series cVOC and ethene mass values measured in selected microcosms inoculated with consortium SDC-9. Symbols for cDCE (red circles), VC (yellow squares), and ethene (green triangles).

Initial acceptance criteria for fitted rate constants required that the 95% confidence interval on the fitted rate constant be equal to or lower than the rate coefficient value itself. However, because the best fit k_{cDCE}, k_{vc}, and global model R^2 are not independent, (i.e., reflect tradeoff between goodness of fit to cDCE and transformation product time-series concentrations subject to mass balance constraints), a more appropriate acceptance criterion was established to require: (1) a global R^2 value of ≥0.75 and (2) an average ratio of the 95% confidence interval on the k_{cDCE} and k_{vc} rate constants of ≥125%. Of the 40 microcosm tests performed (excluding live and killed controls), 28 and 17 tests yielded k_{cDCE} and k_{vc} rate coefficient

https://doi.org/10.1021/acsestengg.1c00207
ACS EST Engg. 2022, 2, 43–53

Table 1. Summary of Fitted Values of k_{cDCE} and k_{vc} in Microcosm Studies[a]

Microcosm Test Replicate	Microcosm Setup	Target *Dhc* Gene Copies mL^{-1}	Initial *Dhc* Gene Copies mL^{-1}	Sampling Schedule	k_{cDCE}, day^{-1}	k_{VC}, day^{-1}	R^2 model
Microcosms Study #1							
Set M1-1A	Groundwater	10^8	$8x10^8$	7 times in 24 hours	62.6 ± 73.1	10.2 ± 3.9	0.85
Set M1-1B	Groundwater	10^8	$5x10^8$	7 times in 24 hours	57.0 ± 53.7	10.2 ± 3.6	0.86
Set M1-1C	Groundwater	10^8	$6x10^8$	7 times in 24 hours	73.6 ± 146.0	11.3 ± 5.9	0.77
Set M1-2A	Groundwater	10^7	$2x10^7$	7 times in 5 days	1.48 ± 0.50	0.31 ± 0.073	0.88
Set M1-2B	Groundwater	10^7	$1x10^7$	7 times in 5 days	1.49 ± 0.48	0.34 ± 0.078	0.89
Set M1-2C	Groundwater	10^7	$2x10^7$	7 times in 5 days	1.68 ± 0.53	0.34 ± 0.070	0.91
Set M1- 3A	Groundwater	10^6	$1x10^5$	11 times in 83 days	0.024 ± 0.0026	0.0015 ± 0.0018	0.90
Set M1-3B	Groundwater	10^6	$2x10^4$	11 times in 83 days	$0.016 \pm 1.2 \bullet 10^{-8}$	$0.00058 \pm 6.6 \bullet 10^{-8}$	0.88
Set M1-3C	Groundwater	10^6	$6x10^5$	11 times in 83 days	$0.026 \pm 2.2 \bullet 10^{-7}$	$0.0037 \pm 6.6 \bullet 10^{-7}$	0.89
Set M1-4A	Groundwater	10^5	$5x10^3$	8 times in 83 days	0.0013 ± 0.00013	--	0.91
Set M1-4B	Groundwater	10^5	$2x10^3$	8 times in 83 days	0.0014 ± 0.0014	0.000001 ± 0.026	0.91
	Microcosm Study #2						
Set M2-1A	Groundwater	10^7	$1x10^7$	9 times in 28 days	1.05 ± 0.94	0.11 ± 0.018	0.94
Set M2-1B	Groundwater	10^7	$2x10^7$	9 times in 28 days	1.05 ± 1.14	0.13 ± 0.028	0.92
Set M2-1C	Groundwater	10^7	$3x10^7$	9 times in 28 days	1.13 ± 1.28	0.17 ± 0.041	0.83
Set M2-1D	Groundwater + Solids	10^2	$5x10^2$	13 times in 42 days	0.14 ± 0.05	0.01 ± 0.008	0.95
Set M2-1D dup	Groundwater + Solids	10^4	$6x10^4$	13 times in 42 days	0.07 ± 0.004	0.0001 ± 0.001	0.95
Set M2-2A	Groundwater	10^6	$4x10^4$	13 times in 42 days	0.0028 ± 0.0004	0.0031 ± 0.0086	0.49
Set M2-2B	Groundwater	10^6	$6x10^3$	13 times in 42 days	0.0018 ± 0.00024	0.0026 ± 0.0083	0.53
Set M2-2C	Groundwater	10^6	$1x10^3$	13 times in 42 days	0.00244 ± 0.00039	0.0042 ± 0.0099	0.34
Set M2-3A	Groundwater + Solids	10^7	$1x10^6$	5 times in 14 days	0.14 ± 0.016	0.019 ± 0.0081	0.97
Set M2-3B	Groundwater + Solids	10^7	$7x10^5$	5 times in 14 days	0.088 ± 0.013	0.018 ± 0.015	0.92
Set M2-3C	Groundwater + Solids	10^7	$4x10^6$	5 times in 14 days	0.096 ± 0.015	0.021 ± 0.015	0.92
	Microcosm Study #3						
Set M3-1A	Groundwater	10^7	$1x10^7$	3 times in 4 days	0.28 ± 0.038	0.013 ± 0.031	0.99
Set M3-1B	Groundwater	10^7	$4x10^6$	3 times in 4 days	0.30 ± 0.031	0.000027 ± 0.023	0.99
Set M3-1C	Groundwater	10^7	$5x10^6$	3 times in 4 days	0.22 ± 0.017	0.0067 ± 0.021	1.00
Set M3-2A	Groundwater + Solids	10^7	$1x10^7$	9 times in 7 days	0.078 ± 0.0046	0.00001 ± 0.016	0.97
Set M3-2B	Groundwater + Solids	10^7	$8x10^6$	9 times in 7 days	0.059 ± 0.0038	0.018 ± 0.020	0.96
Set M3-2C	Groundwater + Solids	10^7	$1x10^7$	9 times in 7 days	0.057 ± 0.0035	0.0027 ± 0.018	0.96

[a]Values in cells shaded in grey were not used in the calcuations of correlation to the biomarkers.

Table 2. Rate Coefficients and Biomarker Correlations

Biomarker Abundance Correlations with Rate Coefficients (Biomarker Abundance, All Microcosm Time Points)									
	OmeA	PceA	TceA	VcrA	*Dhc*_16S rRNA gene	*omeA*	*pceA*	*tceA*	*vcrA*
log k_{cDCE}	0.737	0.571	0.575	0.374	0.844	0.801	0.804	0.859	0.856
p value	2×10^{-7}	6×10^{-6}	1×10^{-6}	6×10^{-3}	2×10^{-7}	2×10^{-7}	2×10^{-7}	2×10^{-7}	2×10^{-7}
n	57	55	62	54	64	64	62	64	64
log k_{VC}	0.774	0.797	0.652	0.678	0.932	0.905	0.91	0.934	0.93
p value	2×10^{-7}	2×10^{-7}	3×10^{-5}	3×10^{-5}	2×10^{-7}	2×10^{-7}	2×10^{-7}	2×10^{-7}	2×10^{-7}
n	35	33	34	30	36	36	36	36	36
Biomarker Abundance Correlations with Rate Coefficients (Biomarker Abundance, Microcosm Mid-Points Only)									
	OmeA	PceA	TceA	VcrA	*Dhc*_16S rRNA gene	*omeA*	*pceA*	*tceA*	*vcrA*
log k_{cDCE}	0.852	0.793	0.755	0.725	0.863	0.881	0.854	0.905	0.918
p value	2×10^{-7}	2×10^{-7}	2×10^{-7}	7×10^{-4}	2×10^{-7}	2×10^{-7}	2×10^{-7}	2×10^{-7}	2×10^{-7}
n	21	21	23	17	23	23	23	23	23
log k_{VC}	0.925	0.836	0.765	0.916	0.934	0.966	0.943	0.953	0.962
p value	2×10^{-7}	2×10^{-7}	4×10^{-4}	2×10^{-7}	2×10^{-7}	2×10^{-7}	2×10^{-7}	2×10^{-7}	2×10^{-7}
n	15	15	15	11	15	15	15	15	15

data that met the quality criteria for further evaluation, respectively (Table 1). The rate constants that provided the best fit to the data collected from the microcosm incubations are presented in Table 1. Reductive dechlorination and ethene formation were not observed in control incubations. The rate

https://doi.org/10.1021/acsestengg.1c00207
ACS EST Engg. 2022, 2, 43−53

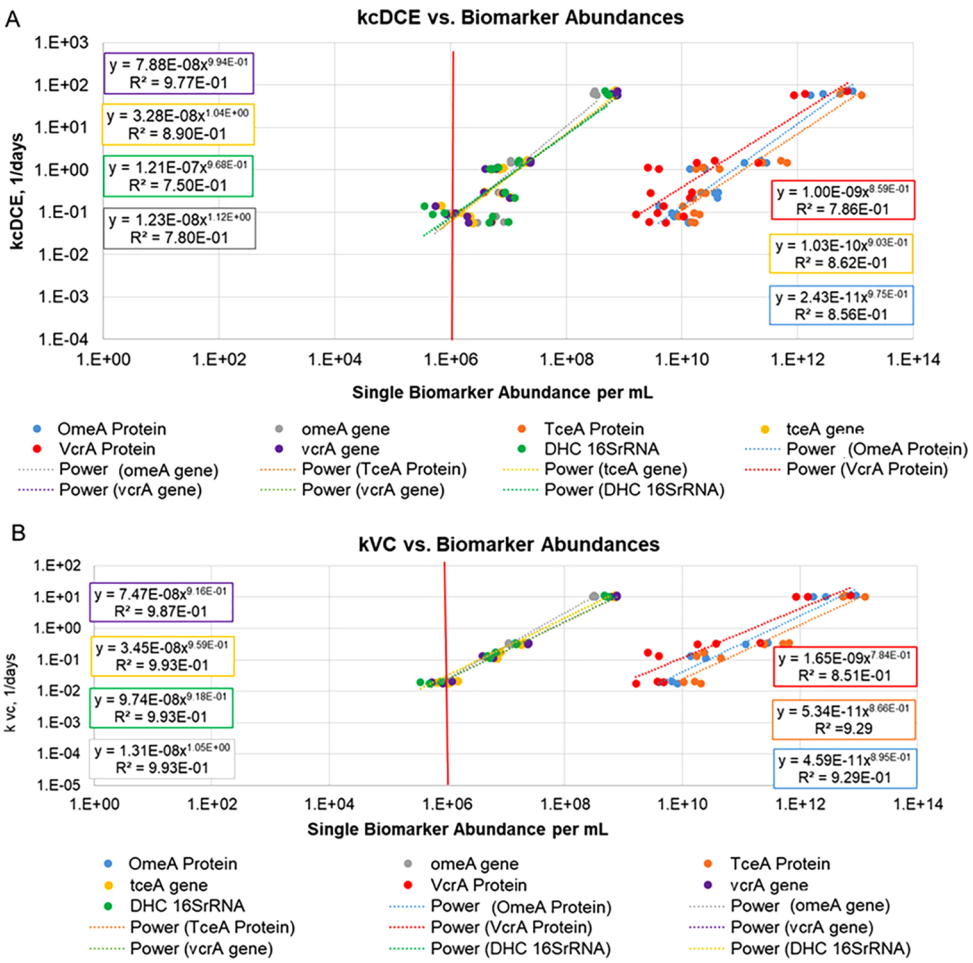

Figure 3. Rate coefficients vs biomarker regression results for cDCE (A) and VC (B). The regression analysis included microcosms that yielded statistically significant rate coefficients, and their corresponding mid-point biomarker gene and protein abundances were used to perform the regression analysis shown above.

constants describe transformation of cDCE and VC by *Dhc* inoculated into the aquifer microcosms.

Genes and Proteins as Predictors of Reductive Dechlorination Rates. Gene and protein abundances collected from early, middle, and late time points from each microcosm positively and significantly correlated with the k_{cDCE} and k_{vc} rate coefficients extracted from those microcosms (Table 2). The correlation coefficients between biomarker abundances and rate coefficients were generally highest when only the middle time point biomarker abundances were included in the correlation analysis. For example, the correlation coefficient for the abundance of the VcrA protein and the k_{cDCE} rate coefficient increased from 0.374 to 0.725 when only the middle time point protein abundances were considered (Table 2). This may reflect the general metabolic status of the dechlorinating *Dhc* cells in the batch system (i.e., *Dhc* bacteria had time to acclimate to the groundwater after inoculation and were actively dechlorinating cDCE). This status may most effectively simulate *in situ* conditions, where electron acceptor (e.g., cDCE) and nutrients are supplied by moving groundwater. Accordingly, the rate coefficient vs biomarker abundances regression analyses were performed using the midpoint biomarker abundances only. The midpoint conditions reflect the steady state *in situ* conditions better than the early and late time points, and here we see the best correlation, which is an encouraging observation and provides strong justification for validation of this approach at field sites.

Rate Coefficients at MNA Sites. Results of the power law least squares regression analysis of cDCE and VC rate coefficients versus gene and protein abundances are presented in Figure 3. The method detection limit for the target proteins TceA and VcrA was 3 fmol, which is equivalent to a typical 1 L groundwater sample containing 2×10^6 proteins/mL.[30] Following the regression trends of target proteins down to the method detection limit would translate to k_{cDCE} and k_{vc} rate constants in the range of 0.0001 per day (~0.04 per year). Prior work indicated that rate constants ≥0.3 per year are "generally useful" for MNA of chlorinated hydrocarbons.[31] While the qProt approach does not reach the level of sensitivity provided by qPCR, qProt is sufficiently sensitive to allow meaningful measurements of biomarker proteins in groundwater with *Dhc* cell abundances exceeding 10^6 *Dhc* cells/mL, assuming that a sufficiently large volume of groundwater is available. The ratio of proteins to 16S rRNA *Dhc* gene in the samples ranged from 1×10^3 to 1×10^5 with an average near 1×10^4 (Figure 3). To effectively extract and quantify RDases with a high degree of confidence, at least 10^6 *Dhc* cells are needed to reach the protein detection limit.

The predictive power of gene and protein biomarker abundances was tested using the regression equations featured in Figure 3 and the biomarker abundance data from

https://doi.org/10.1021/acsestengg.1c00207
ACS EST Engg. 2022, 2, 43−53

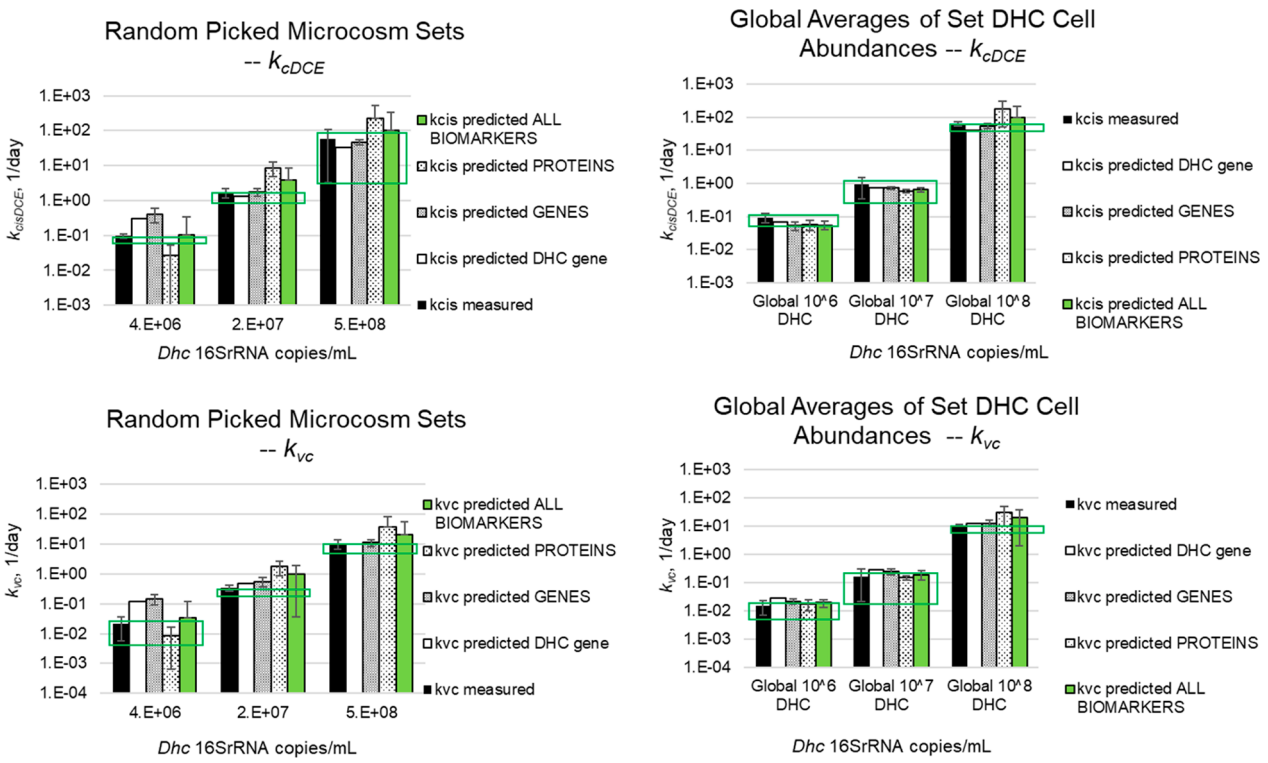

Figure 4. Biomarker-based rate predictions vs measured rate coefficients for (A,C) k_{cDCE} for random picked microcosm sets, and (B, D) k_{VC} for set DHC cell abundances. Green boxes reflect the error range defined as standard deviation associated with the measured rate coefficients determined in this study. Rates predicted using a combination of qPCR and qProt data (green bars) generally yielded an improved rate prediction compared to RDase proteins alone.

microcosm tests that met the data quality acceptance screening criteria (Table 2) but were not included in the regression analysis. The test was performed in two ways (1) using randomly selected biomarker abundances corresponding to a range of *Dhc* cell abundances, and (2) using global averages of all biomarker abundances that corresponded to *Dhc* cell abundances at 10^6, 10^7, and 10^8 cells/mL. The randomly selected biomarker abundances corresponded to the time zero sampling from microcosm set M1-1B, set M1-2C, and set M2-3C. As shown in Figure 3, qProt-based rate predictions (white bars with black dots) were within an order of magnitude of measured rate coefficients (green boxes) for all tests. Rates predicted using a global average abundance of all genes and proteins (green bars, Figure 4) were generally better than those predicted by qProt alone.

Data Integration and Environmental Relevance. Microcosm rate coefficients (Table 1) were positively and significantly correlated with both DNA- and protein biomarker abundances (Table 2). Protein- and gene-based rate predictions were within an order of magnitude of the measured rate coefficients (green boxes) for all tests (Figure 3). At low *Dhc* cell titers in the randomly selected microcosms, the rate constants predicted from the abundance of gene biomarkers were higher than the measured rate constants and the rate constants predicted from the abundance of proteins. At intermediate and higher abundances of *Dhc* in the randomly selected microcosms, the rate constants predicted from the qPCR measurements matched the measured rate constants and were equal to or less than the rate constants predicted from qProt. Rates predicted using a combination of genes and proteins (green bars, Figure 4) generally resulted in the best match with the measured rate constants and were statistically different for qProt as demonstrated by the Spearman test (Figure S15). The reasons why the combined measurements of qPCR and qProt resulted in the best fit and best matched the measured rate coefficients are unclear but may be related to the largely unexplored regulatory controls of gene expression and biomarker protein (e.g., RDase) turnover in *Dhc*. While these questions warrant further investigation, the findings imply that the combined measurements of biomarker genes with qPCR and proteins with qProt provide a means to generate reasonable estimates of *in situ* rate coefficients. Considering the difficulty in obtaining *in situ* rate estimates for contaminant degradation using conventional methodologies and the uncertainty associated with these rate calculations, the new approach described herein offers a viable alternative to more rapidly and cost-efficiently generate meaningful rate estimates, on which site management decision making decisions can be based.

The laboratory microcosm test system was appropriate for demonstrating a quantitative relationship between biomarker abundances and RD rates mediated by *Dhc* cells present in the SDC-9 consortium. Of course, batch microcosms do not perfectly emulate *in situ* conditions at cVOC-contaminated aquifers and follow up studies at field sites are needed to validate the application of molecular approaches to generate meaningful rate estimates.

A prior study demonstrated that a substantial portion of *Dhc* cells is attached to the aquifer solids during RD activity and that the proportion of attached *Dhc* cells is generally higher in aquifers with higher organic carbon content and during active growth of *Dhc*.[32] This implies that sampling only the groundwater may not reveal the absolute abundance of *Dhc* cells in an aquifer and underestimates of the true RD activity

https://doi.org/10.1021/acsestengg.1c00207
ACS EST Engg. 2022, 2, 43−53

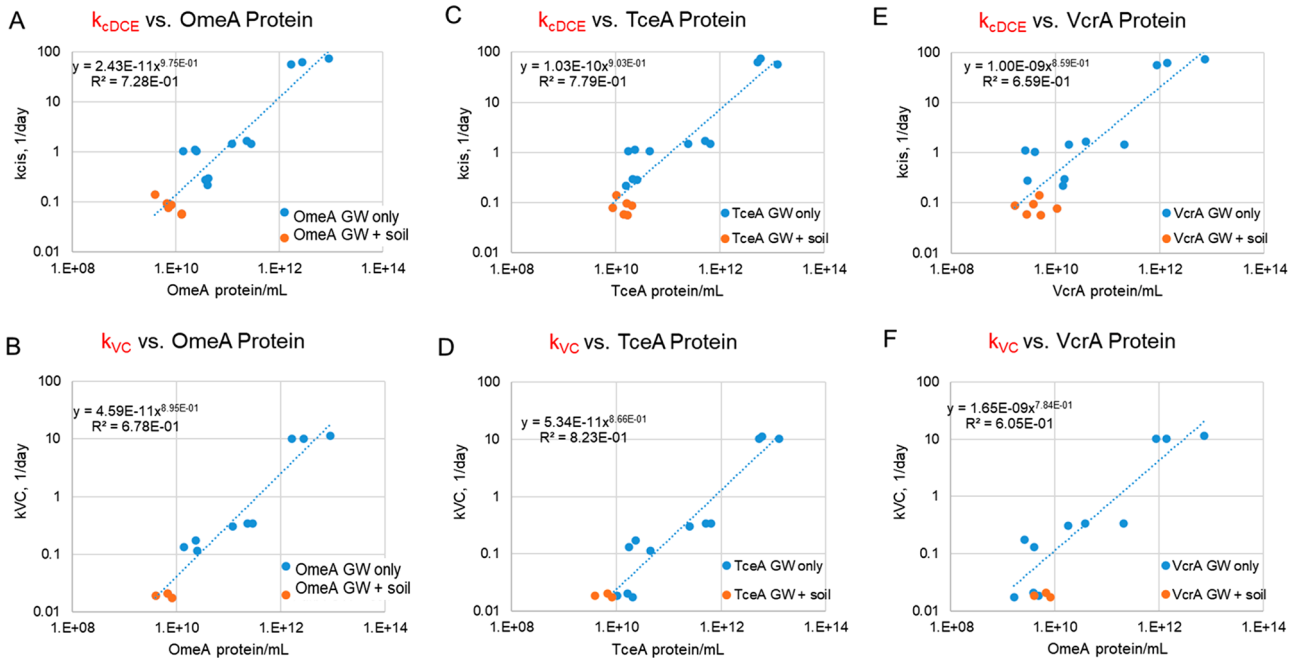

Figure 5. Rate coefficients vs biomarker abundances with treatments. Relationship between rate of cDCE and VC degradation is plotted for proteins: OmeA (panels A and B), TceA (panels C and D), and VcrA (panels E and F). Blue and orange symbols represent biomarker and rate coefficient results from groundwater-only microcosms and groundwater with aquifer solids microcosms, respectively.

are possible. Schaefer et al.[33] showed in parallel batch microcosms and continuous flow column studies that aqueous-phase *Dhc* could be used to estimate RD rates and that batch studies with sediments dramatically underestimated RD activity compared to more relevant flow-through conditions. The majority of the bioaugmented microcosm tests in our work featured only groundwater; relatively few microcosms featured groundwater with aquifer solids. Results of the rate coefficient vs protein biomarker abundance regressions are reproduced in Figure 5 below, here with the groundwater-only (blue symbols) and groundwater with aquifer material (orange symbols) differentiated for each biomarker. The data from the microcosms that featured groundwater with soil, generally clustered at the low end of the biomarker abundances and RD rates. Although the microcosms with aquifer material tended to have lower biomarker abundances and RD activities, the results were generally consistent with the entirety of the data set, suggesting no significant difference in the presence of aquifer solids on the relationship between the abundance of the RDase proteins in the water and the measured rate constant for degradation.

Second, in a natural aquifer system, the abundance of bacteria will adjust to a level where growth sustained by the supply of the limiting resource (e.g., cDCE, inorganic nutrients, or electron donor) is balanced by cell decay. Indeed, viable microbes present in a natural system consume dead cells (necromass) as a nutrient source.[34] The turnover of necromass in natural systems will, in theory, minimize the chance of detecting "carcass proteins" (in this case biomarkers associated with dead *Dhc* cells). While the presence of such biomarker proteins in nonviable cells would be difficult to quantify, we did evaluate whether the protein levels detected were reasonable based on the abundance of *Dhc* DNA measured. If protein to *Dhc* cell abundances were greater than physiologically expected, or if ratios were much higher than have been previously published for RDase proteins in *Dhc*, the presence of RDases not associated with viable cells could be a confounding factor in RDase biomarker vs rate coefficient regressions established in this study. Observed ratios were generally between 10^3 and 10^5 proteins/cell (Figure 3), which is in the range of previously published values of 7.6×10^3 and 2.60×10^4 for TceA reported for *Dhc* cells in the KB-1 and D2 cultures, respectively[30] Further, the theoretical maximum number of proteins that could fit in the periplasmic space of a *Dhc* cell was estimated to be 10^5 proteins.[33,34] If 10% of the membrane-associated proteins in a *Dhc* cell are RDases, the maximum number of RDases per *Dhc* cell would be 10^4. Therefore, the observed range of RDase proteins per *Dhc* cell during this study is in the range of prior observations and within the physical boundaries of a *Dhc* cell.

Finally, because first order-based kinetics often describe RD at field scales reasonably well, our first order-based regressions (Figures 3 and 5) based on qProt and qPCR data will be directly applicable at many field sites. In a natural system, *Dhc* abundance will adjust to a level where growth controlled by the supply of chlorinated ethenes is balanced by decay. In this case, the abundance of *Dhc* and concentration of chlorinated ethenes remain relatively constant at any one position along the flow path. In such cases, cVOC degradation kinetics can be described by a pseudo first-order kinetic model, i.e., at any one location along the flow path, the overall rate of degradation of the substrate (i.e., the contaminant) in the groundwater (μg/L per day) divided by the concentration of the substrate (μg/L) is a fixed ratio.

CONCLUSIONS

The ability to predict *in situ* rate constants for cVOC biodegradation in aquifers from biological and/or geochemical measures obtained from groundwater samples has remained elusive. Rather, such predictions typically rely on monitoring and modeling long-term plume behavior and analyzing groundwater samples over a period of years to provide

https://doi.org/10.1021/acsestengg.1c00207
ACS EST Engg. 2022, 2, 43−53

secondary evidence that conditions are conducive for RD. This time-consuming approach is currently necessary to establish and support MNA remedies at cVOC sites and difficult and expensive to implement in a reasonable timeframe at sites lacking appropriate infrastructure (e.g., wells). The data from this study show that targeted qProt can quantify protein biomarkers over a wide range of *Dhc* cell densities and that protein abundances can predict RD rates. Protein detection limits translated to a rate coefficient of 10^{-4} day^{-1} (0.04 $year^{-1}$) for both k_{cDCE} and k_{vc}, which is within the range observed at sites undergoing MNA. The combined analysis of both qProt and qPCR biomarker data resulted in the best match with the measured rate constants of cDCE and VC biodegradation in the test microcosms. These laboratory findings suggest that quantitative biomarker measurements, particularly the combination of protein- and gene-centric quantitative measurements, may be useful to rapidly predict *in situ* RD rates, which would represent a major advance for cost-effective site management.

The microcosm studies conducted for this project to correlate rates of cVOC biodegradation with RDase abundance were extensive and would not be required for field implementation. Except for metagenomics and metaproteomics, the techniques used to assess contaminant degradation and continued potential for natural attenuation are common and costs to apply these techniques are well documented in the literature. Many of these techniques have only limited commercial availability and/or are available through a university or other research laboratory. As such, application costs remain relatively high. It is expected that as these techniques mature, they will become more widely available and the analytical cost per sample will decrease substantially. For comparison purposes, the cost of shotgun and quantitative metaproteomic analyses based on cost data collected during this demonstration were $800 and $200 per sample, respectively, assuming analysis of a batch of 12 samples. The cost of the metaproteomic analyses included use of an existing metaproteomic platform but assumed development of a workflow specific for cVOCs.

■ ASSOCIATED CONTENT

Supporting Information

The Supporting Information is available free of charge at https://pubs.acs.org/doi/10.1021/acsestengg.1c00207.

> Description of methods for detection and characterization of respiratory RDases, standard geochemical cVOC analyses, DNA extraction, and qPCR and the qProt; tables on specific qPCR primers for all gene targets as well as their amplification efficiencies (Tables S1 and S2); method detection limit and sequences of peptides for qProt assay (Table 3); relationship among RDases from sequenced environmental samples in relation to the SDC-9 metagenome (Figure S1) (PDF)

■ AUTHOR INFORMATION

Corresponding Author

Katarzyna H. Kucharzyk − *Battelle Memorial Institute, Columbus, Ohio 43201, United States;* orcid.org/0000-0001-8524-2989; Email: kucharzyk@battelle.org

Authors

Mandy M. Michalsen − *U.S. Army Engineer Research and Development Center, Environmental Laboratory, Vicksburg, Mississippi 39180, United States*

Fadime Kara Murdoch − *Battelle Memorial Institute, Columbus, Ohio 43201, United States; Center for Environmental Biotechnology, Department of Microbiology, Department of Civil and Environmental Engineering, and Department of Biosystems Engineering and Soil Science, University of Tennessee, Knoxville, Tennessee 37996, United States*

Frank E. Löffler − *Center for Environmental Biotechnology, Department of Microbiology, Department of Civil and Environmental Engineering, and Department of Biosystems Engineering and Soil Science, University of Tennessee, Knoxville, Tennessee 37996, United States; Biosciences Division, Oak Ridge National Laboratory, Oak Ridge, Tennessee 37831, United States;* orcid.org/0000-0002-9797-4279

John Wilson − *Scissortail Environmental Solutions, LLC, Ada, Oklahoma 74820, United States*

Paul B. Hatzinger − *Aptim Federal Services, LLC, Lawrenceville, New Jersey 08648, United States*

Jack D. Istok − *School of Civil and Construction Engineering, Oregon State University, Corvallis, Oregon 97331, United States*

Larry Mullins − *Battelle Memorial Institute, Columbus, Ohio 43201, United States*

Amy Hill − *Battelle Memorial Institute, Columbus, Ohio 43201, United States*

Robert W. Murdoch − *Battelle Memorial Institute, Columbus, Ohio 43201, United States*

Charles Condee − *Aptim Federal Services, LLC, Lawrenceville, New Jersey 08648, United States*

Complete contact information is available at: https://pubs.acs.org/10.1021/acsestengg.1c00207

Notes

The authors declare no competing financial interest.

■ ACKNOWLEDGMENTS

This research was funded by the Environmental Security & Technology Certification Program (ESTCP) and by USACE Louisville District under contract W912DW17P0036. We wish to thank several APTIM scientists for assisting in the studies including Simon Vainberg for growing the SDC-9 culture, Sheryl Streger for assisting in sample collection, and Anthony Soto and Paul Hedman for performing analytical work. We would also like to thank Mr. Jacob Lalley and Mr. Tanner Reliford (USACE ERDC and USACE Louisville District, respectively) for their support and leadership during field sample collection.

■ REFERENCES

(1) EPA, U., *Superfund Remedy Report*; 16th Edition. EPA, 2020.

(2) Mattes, T. E.; Jin, Y. O.; Livermore, J.; Pearl, M.; Liu, X. Abundance and activity of vinyl chloride (VC)-oxidizing bacteria in a dilute groundwater VC plume biostimulated with oxygen and ethene. *Appl. Microbiol. Biotech.* **2015**, *99*, 9267−9276.

(3) Ritalahti, K.; Cruz-García, C.; Padilla-Crespo, E.; Hatt, J.; Löffler, F., RNA extraction and cDNA analysis for quantitative assessment of biomarker transcripts in groundwater. In *Handbook of Hydrocarbon*

and Lipid Microbiology; Springer 2010. pp. 3671−3685, DOI: 10.71007/978-3-540-77587-4_289
(4) Vainberg, S.; Condee, C. W.; Steffan, R. J. Large-scale production of bacterial consortia for remediation of chlorinated solvent-contaminated groundwater. *J. Ind. Microbiol. Biotechnol.* **2009**, *36*, 1189−1197.
(5) Löffler, F. E.; Yan, J.; Ritalahti, K. M.; Adrian, L.; Edwards, E. A.; Konstantinidis, K. T.; Müller, J. A.; Fullerton, H.; Zinder, S. H.; Spormann, A. M. *Dehalococcoides mccartyi* gen. nov., sp. nov., obligately organohalide-respiring anaerobic bacteria relevant to halogen cycling and bioremediation, belong to a novel bacterial class, *Dehalococcoidia* classis nov., order *Dehalococcoidales* ord. nov. and family *Dehalococcoidaceae* fam. nov., within the phylum Chloroflexi. *Int. J. System. Evolut. Microbiol.* **2013**, *63*, 625−635.
(6) Hatt, J. K.; Ritalahti, K. M.; Ogles, D. M.; Lebrón, C. A.; Löffler, F. E. Design and application of an internal amplification control to improve Dehalococcoides mccartyi 16S rRNA gene enumeration by qPCR. *Environ. Sci. Technol.* **2013**, *47*, 11131−11138.
(7) Molenda, O.; Jácome, L. A. P.; Cao, X.; Nesbø, C. L.; Tang, S.; Morson, N.; Patron, J.; Lomheim, L.; Wishart, D. S.; Edwards, E. A. Insights into origins and function of the unexplored majority of the reductive dehalogenase gene family as a result of genome assembly and ortholog group classification. *Environ. Sci. Proc. Impacts* **2020**, *22*, 663−678.
(8) Hatt, J. K.; Löffler, F. E. Quantitative real-time PCR (qPCR) detection chemistries affect enumeration of the *Dehalococcoides* 16S rRNA gene in groundwater. *J. Microbiol. Methods* **2012**, *88*, 263−270.
(9) Low, A.; Shen, Z.; Cheng, D.; Rogers, M. J.; Lee, P. K. H.; He, J. A comparative genomics and reductive dehalogenase gene transcription study of two chloroethene-respiring bacteria, *Dehalococcoides mccartyi* strains MB and 11a. *Sci. Reports* **2015**, *5*, 1−12.
(10) Michalsen, M.; Kucharzyk, K.; Bartling, C.; Meisel, J.; Hatzinger, P.; Wilson, J.; Solutions, S. E.; Istok, L. J.; Murdoch, F. K.; Löffler, F., *Validation of Advanced Molecular Biological Tools to Monitor Chlorinated Solvent Bioremediation and Estimate cVOC Degradation Rates ESTCP Report* ER 201726, March 24, 2020. 2020.
(11) Chourey, K.; Jansson, J.; VerBerkmoes, N.; Shah, M.; Chavarria, K. L.; Tom, L. M.; Brodie, E. L.; Hettich, R. L. Direct cellular lysis/protein extraction protocol for soil metaproteomics. *J. Proteome Res.* **2010**, *9*, 6615−6622.
(12) Kublik, A.; Deobald, D.; Hartwig, S.; Schiffmann, C. L.; Andrades, A.; von Bergen, M.; Sawers, R. G.; Adrian, L. Identification of a multi-protein reductive dehalogenase complex in *Dehalococcoides mccartyi* strain CBDB1 suggests a protein-dependent respiratory electron transport chain obviating quinone involvement. *Environ. Microbiol.* **2016**, *18*, 3044−3056.
(13) Steffan, R. J.; Vainberg, S., Production and handling of *Dehalococcoides* bioaugmentation cultures. In *Bioaugmentation for groundwater remediation*; Springer: 2013; pp. 89−115, DOI: 10.1007/978-1-4614-4115-1_3.
(14) Kucharzyk, K. H.; Meisel, J. E.; Kara-Murdoch, F.; Murdoch, R. W.; Higgins, S. A.; Vainberg, S.; Bartling, C. M.; Mullins, L.; Hatzinger, P. B.; Löffler, F. E. Metagenome-guided proteomic quantification of reductive dehalogenases in the *Dehalococcoides mccartyi*-containing consortium SDC-9. *J. Proteome Res.* **2020**, *19*, 1812−1823.
(15) Ritalahti, K. M.; Amos, B. K.; Sung, Y.; Wu, Q.; Koenigsberg, S. S.; Löffler, F. E. Quantitative PCR targeting 16S rRNA and reductive dehalogenase genes simultaneously monitors multiple *Dehalococcoides* strains. *Appl. Environ. Microbiol.* **2006**, *72*, 2765−2774.
(16) Johnson, D. R.; Lee, P. K. H.; Holmes, V. F.; Alvarez-Cohen, L. An internal reference technique for accurately quantifying specific mRNAs by real-time PCR with application to the tceA reductive dehalogenase gene. *Appl. Environ. Microbiol.* **2005**, *71*, 3866−3871.
(17) He, J.; Ritalahti, K. M.; Aiello, M. R.; Löffler, F. E. Complete detoxification of vinyl chloride by an anaerobic enrichment culture and identification of the reductively dechlorinating population as a *Dehalococcoides* species. *Appl. Env. Microbiol.* **2003**, *69*, 996−1003.
(18) Seidel, K.; Kühnert, J.; Adrian, L. The complexome of *Dehalococcoides mccartyi* reveals its organohalide respiration-complex is modular. *Front. Microbiol.* **2018**, *9*, 1130.
(19) Price, M. N.; Dehal, P. S.; Arkin, A. P. FastTree 2 − Approximately maximum-likelihood trees for large alignments. *PLoS One* **2010**, *5*, e9490−e9490.
(20) Bolger, A. M.; Lohse, M.; Usadel, B. Trimmomatic: a flexible trimmer for Illumina sequence data. *Bioinformatics* **2014**, *30*, 2114−2120.
(21) Menzel, P.; Ng, K. L.; Krogh, A. Fast and sensitive taxonomic classification for metagenomics with Kaiju. *Nat. Commun.* **2016**, *7*, 11257.
(22) Bankevich, A.; Nurk, S.; Antipov, D.; Gurevich, A. A.; Dvorkin, M.; Kulikov, A. S.; Lesin, V. M.; Nikolenko, S. I.; Pham, S.; Prjibelski, A. D.; Pyshkin, A. V.; Sirotkin, A. V.; Vyahhi, N.; Tesler, G.; Alekseyev, M. A.; Pevzner, P. A. SPAdes: A New Genome Assembly Algorithm and Its Applications to Single-Cell Sequencing. *J. Comput. Biol.* **2012**, *19*, 455−477.
(23) Gurevich, A.; Saveliev, V.; Vyahhi, N.; Tesler, G. QUAST: quality assessment tool for genome assemblies. *Bioinformatics* **2013**, *29*, 1072−1075.
(24) Chen, I. M. A.; Chu, K.; Palaniappan, K.; Pillay, M.; Ratner, A.; Huang, J.; Huntemann, M.; Varghese, N.; White, J. R.; Seshadri, R.; Smirnova, T.; Kirton, E.; Jungbluth, S. P.; Woyke, T.; Eloe-Fadrosh, E. A.; Ivanova, N. N.; Kyrpides, N. C. IMG/M v. 5.0: an integrated data management and comparative analysis system for microbial genomes and microbiomes. *Nucleic Acids Res.* **2019**, *47*, D666−D677.
(25) Aziz, C.; Newell, C.; Gonzales, J.; Haas, P.; Clement, T.; Sun, Y., *BIOCHLOR Natural Attenuation Decision Support System*; User's Manual Version 1.0. US Environmental Protection Agency 2000.
(26) Sabalowsky, A. R.; Semprini, L. Trichloroethene and cis-1, 2-dichloroethene concentration-dependent toxicity model simulates anaerobic dechlorination at high concentrations: I. batch-fed reactors. *Biotechnol. Bioeng.* **2010**, *107*, 529−539.
(27) Smith, L. H.; McCarty, P. L.; Kitanidis, P. K. Spreadsheet method for evaluation of biochemical reaction rate coefficients and their uncertainties by weighted nonlinear least-squares analysis of the integrated Monod equation. *Appl. Environ. Microbiol.* **1998**, *64*, 2044−2050.
(28) Royston, P. Approximating the Shapiro-Wilk W-test for non-normality. *Stat. Comput.* **1992**, *2*, 117−119.
(29) Solis, M. I. V.; Abraham, P. E.; Chourey, K.; Swift, C. M.; Löffler, F. E.; Hettich, R. L. Targeted detection of Dehalococcoides mccartyi microbial protein biomarkers as indicators of reductive dechlorination activity in contaminated groundwater. *Sci. Rep.* **2019**, *9*, 1−11.
(30) Werner, J. J.; Ptak, A. C.; Rahm, B. G.; Zhang, S.; Richardson, R. E. Absolute quantification of *Dehalococcoides* proteins: enzyme bioindicators of chlorinated ethene dehalorespiration. *Environ. Microbiol.* **2009**, *11*, 2687−2697.
(31) Lu, X.; Wilson, J. T.; Kampbell, D. H. Relationship between *Dehalococcoides* DNA in ground water and rates of reductive dechlorination at field scale. *Water Res.* **2006**, *40*, 3131−3140.
(32) Abriola, L. M.; Capiro, N. L.; Christ, J. A.; Chu, L.; Miller, E. L.; Pennell, K. D. *Development of an Integrated Field Test/Modeling Protocol for Efficient In Situ Bioremediation Design and Performance Uncertainty Assessment*; Tufts University Medford United States: 2019.
(33) Schaefer, C. E.; Condee, C. W.; Vainberg, S.; Steffan, R. J. Bioaugmentation for chlorinated ethenes using *Dehalococcoides sp.* : Comparison between batch and column experiments. *Chemosphere* **2009**, *75*, 141−148.
(34) Dong, X.; Greening, C.; Brüls, T.; Conrad, R.; Guo, K.; Blaskowski, S.; Kaschani, F.; Kaiser, M.; Laban, N. A.; Meckenstock, R. U. Fermentative Spirochaetes mediate necromass recycling in anoxic hydrocarbon-contaminated habitats. *ISME J.* **2018**, *12*, 2039−2050.

https://doi.org/10.1021/acsestengg.1c00207
ACS EST Engg. 2022, 2, 43−53